

# Inferior vena caval hemodynamics quantified in vivo at rest and during cycling exercise using magnetic resonance imaging

Christopher P. Cheng,<sup>1</sup> Robert J. Herfkens,<sup>2</sup> and Charles A. Taylor<sup>1,3</sup>

Departments of <sup>1</sup>Mechanical Engineering, <sup>2</sup>Radiology, and <sup>3</sup>Surgery,  
Stanford University, Stanford, California 94305-3030

Submitted 25 July 2002; accepted in final form 2 December 2002

**Cheng, Christopher P., Robert J. Herfkens, and Charles A. Taylor.** Inferior vena caval hemodynamics quantified in vivo at rest and during cycling exercise using magnetic resonance imaging. *Am J Physiol Heart Circ Physiol* 284: H1161–H1167, 2003. First published December 5, 2002; 10.1152/ajpheart.00641.2002.—Compared with the abdominal aorta, the hemodynamic environment in the inferior vena cava (IVC) is not well described. With the use of cine phase-contrast magnetic resonance imaging (MRI) and a custom MRI-compatible cycle in an open magnet, we quantified mean blood flow rate, wall shear stress, and cross-sectional lumen area in 11 young normal subjects at the supraceliac and infrarenal levels of the aorta and IVC at rest and during dynamic cycling exercise. Similar to the aorta, the IVC experienced significant increases in blood flow and wall shear stress as a result of exercise, with greater increases in the infrarenal level compared with the supraceliac level. At the infrarenal level during resting conditions, the IVC experienced higher mean flow rate than the aorta ( $1.2 \pm 0.5$  vs.  $0.9 \pm 0.4$  l/min,  $P < 0.01$ ) and higher mean wall shear stress than the aorta ( $2.0 \pm 0.6$  vs.  $1.3 \pm 0.6$  dyn/cm<sup>2</sup>,  $P < 0.005$ ). During exercise, wall shear stress remained higher in the IVC compared with the aorta, although not significantly. It was also observed that, whereas the aorta tapers inferiorly, the IVC tapers superiorly from the infrarenal to the supraceliac location. The hemodynamic and anatomic data of the IVC acquired in this study add to our understanding of the venous circulation and may be useful in a clinical setting.

blood flow rate; wall shear stress; lumen area; functional flow imaging

THE VENOUS SYSTEM of the human body, although largely anatomically parallel with the arterial system, is physiologically vastly different from the arterial environment. The venous system, which brings deoxygenated blood from the tissues of the body back to the right side of the heart, is subjected to much lower blood pressures and less flow pulsatility compared with the arterial system (11a, 21). Not surprisingly, the cellular and structural content of venous tissue is vastly different from that of the arteries (1, 21, 24). While there have been a number of detailed hemodynamic studies of the aorta and major arteries, far fewer have been done in the major veins, such as the inferior vena cava (IVC). For example, it has been shown in vivo, in vitro, and with computer simulations that exercise conditions

significantly alter the hemodynamic environment in the abdominal aorta (15–17, 22, 27, 28); however, no similar investigations have been performed for the IVC.

In the arterial system, hemodynamic conditions are hypothesized to play an important role in the localization of atherosclerosis. However, in the major veins, which are far less prone to atherosclerotic disease, hemodynamic quantities have not been adequately documented. It is hypothesized that low flow rate, flow recirculation, low mean wall shear stress, and oscillations in shear stress play a role in the localization of atherosclerotic lesions in the carotid bifurcation, coronary arteries, and abdominal aorta (2, 8, 14, 33). Additionally, it has been shown that lower limb exercise modulates these unfavorable hemodynamic conditions in the abdominal aorta, thereby providing mechanisms by which exercise could delay or combat atherosclerosis development in the aorta and lower extremities (15, 17, 22, 27, 28). From a disease research standpoint, description of the hemodynamic environment in the large veins would help elucidate some of the protective mechanisms by which the venous system is less susceptible to atherosclerosis.

There are also clinical applications for quantifying hemodynamic conditions in the venous system at rest and during exercise. First, phlebography is not as effective in investigating the veins as arteriography is for arteries. Whereas arteriography can generally localize disease with one exam, phlebography often requires many exams with multiple injection sites due to the converging direction of blood flow from branches to trunk. Schanzer et al. (23) found that phlebography only detected 23% of proven cases of regurgitation and that obstruction observed on phlebogram did not necessarily indicate functional obstruction. Flow measurements in the IVC have also shown promise in evaluating venous regurgitation (23) and liver function (29) in adults and assessing renal function (13) and Fontan procedure success (5) in pediatric cases. With the added functionality of measuring IVC hemodynamics during exercise, the capabilities of these diagnostic and therapeutic assessment exams could potentially increase. Measurement of flow conditions in the IVC

Address for reprint requests and other correspondence: C. A. Taylor, Division of Biomechanical Engineering, Durand Bldg., Rm. 213, Stanford, CA 94305-3030 (E-mail: taylorca@stanford.edu).

The costs of publication of this article were defrayed in part by the payment of page charges. The article must therefore be hereby marked "advertisement" in accordance with 18 U.S.C. Section 1734 solely to indicate this fact.

during exercise could also improve device design and treatment planning. For example, venous filters could be better designed to accommodate for exercise flow conditions, and venous bypass grafts could be sized specifically for individual subjects.

To study in vivo hemodynamic conditions such as flow rate, wall shear stress, and lumen area for circulation physiology, disease research, and clinical applications, a noninvasive imaging modality must be utilized. Blood flow can be measured noninvasively and without ionizing radiation by Doppler ultrasound and magnetic resonance imaging (MRI). Doppler ultrasound is an echo-imaging modality that enables measurement of the component of motion in the direction of the insonifying field (10). Although Doppler ultrasound can quantify peak blood velocity and acceleration components reliably, volume flow rates can only be estimated by these velocities and vessels geometries. Additionally, ultrasound cannot measure spatial distributions of through-plane velocity over a cross section. Phase-contrast MRI methods can concurrently acquire accurate, coregistered velocity and anatomic maps for quantification of flow rate, circumferentially resolved wall shear stress, and lumen area (4, 18, 19).

Blood flow rate has previously been measured in the human abdominal aorta using MRI at rest and during lower limb exercise (17, 22, 27), showing significant increases in blood flow during exercise. In addition, Taylor et al. (27) quantified wall shear stress using a method described in Cheng et al. (4), demonstrating statistically higher mean shear stresses during exercise and elimination of shear stress oscillations present at rest. In the IVC of humans, blood flow and lumen area have been measured at rest using MRI (5, 6, 9, 30) and at rest using Doppler ultrasound (11, 26, 30), and blood flow has been measured during plantar and dorsiflexion exercise using strain gauge plethysmography (23). However, quantification of blood flow, wall shear stress, and lumen cross-sectional area have not been performed in the IVC during lower limb exercise.

With the use of a custom MR-compatible stationary cycle in an open magnet and cine phase-contrast MRI techniques (18), we measured blood flow velocities in the IVCs of young healthy subjects at rest and during upright dynamic lower limb exercise. We quantified mean blood flow rate, wall shear stress, and lumen area at the supraceliac and infrarenal levels of the aorta and IVC at these two physiological conditions. We hypothesized that oscillations of flow and wall shear stress that exist in the infrarenal aorta at rest do not exist in the infrarenal IVC and that the increases in flow and wall shear stress observed in the aorta as a result of lower limb exercise also occur in the IVC.

## MATERIALS AND METHODS

Eleven healthy nonsmoking subjects (6 men and 5 women, mean age 23.6 yr, range 20–28 yr) were imaged at rest and during lower limb exercise in a 0.5-T open magnet (GE Signa SP, GE Medical Systems; Milwaukee, WI). None of the subjects had any history of cardiovascular disease. Our human subjects protocol was approved by the Stanford University

Panel on Human Subjects in Medical Research. Each subject was firmly strapped to an upright seat in the open magnet to permit full range of leg motion while positioning the abdomen in the center of the magnet for optimal imaging (Fig. 1). A custom-built MR-compatible cycle was then positioned, and its resistance was adjusted to promote comfortable pedaling and minimize abdomen movement.

Imaging studies were performed at rest and during steady-state lower limb exercise conditions (150% of resting heart rate). During exercise, subjects monitored their own heart rate (monitored by plethysmography) and adjusted the pedaling speed as necessary to maintain a constant heart rate. Cine phase-contrast MRI techniques (18) were used to acquire spatial maps of anatomy (magnitude of signal) and through-plane blood flow velocity (phase of signal) at the supraceliac and infrarenal levels at both physiological states. Image acquisitions were gated to the cardiac cycle with a plethysmograph placed on the right index finger, and the image data were retrospectively reconstructed to 16 evenly spaced time points in the cardiac cycle. The subjects breathed normally during image acquisition, and respiratory compensation algorithms were utilized to account for respiratory motion (7). The scan parameters were as follows: time of repetition = 25 ms, echo time = 9 ms, flip angle = 30°, slice thickness = 5 or 10 mm (depending on the anatomy of the subject), square field of view = 28 × 28 cm, matrix dimensions = 256 × 128 pixels, and through-plane velocity encoding gradient = 150 cm/s.

With the use of the anatomic and velocity data, we quantified volume flow rate, wall shear stress, and lumen cross-sectional area at the supraceliac (immediately superior to the celiac trunk on the aorta) and infrarenal (inferior to the renal



Fig. 1. A subject pedaling the custom-built magnetic resonance compatible stationary cycle with the GE 0.5-T open magnet.

arteries and veins) levels of the IVC. For the flow calculation, the cross section of the IVC was isolated by threshold segmentation of the magnitude data, the phase data were adjusted with a second-order baseline correction, and blood flow velocities associated with each pixel within the cross section were integrated to calculate total volume flow rate (19).

Wall shear stress computation requires an accurate segmentation of the lumen boundary, estimation of the fluid shear rate along that boundary, and a value for blood dynamic viscosity. We used a curvature-constrained level set method to identify curve *C*, which is the boundary of the lumen in the imaging plane (25, 31). Velocities outside of the curve *C* are set to zero. To estimate the shear rate on curve *C*, we constructed a band of two-dimensional elements along the inside of the lumen. The elements are composed of third-order Lagrangian shape functions that represent the velocity surface of the blood flow near the vessel wall. The velocities at the element nodes are determined by bicubic interpolation of the surrounding 16 pixels on the phase image. Velocities, at any point on the elements, are then defined as the sum of the products of the Lagrangian interpolation functions evaluated at this point and the corresponding element nodal velocities. From the velocity surface, the velocity gradient vector is computed along the circumference of the lumen and dotted with the corresponding unit normal vector to curve *C*. Finally, we computed the wall shear stress ( $\tau$ ) using the equation

$$\tau = \mu \left( \frac{\partial v}{\partial x} \mathbf{n}_x + \frac{\partial v}{\partial y} \mathbf{n}_y \right)$$

where *v* is the through-plane blood velocity, ( $\mathbf{n}_x$ ,  $\mathbf{n}_y$ ) are the *x* and *y* components of the unit normal vector to curve *C*, and  $\mu$  is the dynamic viscosity of the blood (taken to be 4 cP). This method has been described in detail and validated with software and in vitro flow phantoms in previous studies (3, 4). Lumen area was computed from the level set segmentation mentioned above.

Blood flow rate and lumen area are presented as temporally averaged over the cardiac cycle. The wall shear stress data are presented as circumferentially averaged along the luminal curve and temporally averaged over the cardiac cycle. Average population data are presented as means  $\pm$ SD. Statistical significance was determined by paired *t*-tests accompanied by ANOVA and Bonferroni correction for multiple comparisons where appropriate. A confidence level of 95% was considered significant.

## RESULTS

Heart rate increased from  $73 \pm 6.2$  beats/min at rest to  $110 \pm 8.8$  beats/min during exercise ( $P < 0.0001$ ) in our 11 subjects. The transition in physiological state from rest to lower limb exercise also resulted in significant changes in the blood flow environment for both the IVC and abdominal aorta.

Figure 2 depicts volumetric flow rate and through-plane velocity data for the supraceliac (*top*) and infrarenal (*bottom*) levels of the abdominal aorta and IVC at rest (*left*) and during exercise (*right*) for a representative subject. As seen in the flow rate curves versus time, blood flow is much more pulsatile in the abdominal aorta compared with the IVC at both anatomic locations and physiological states (Fig. 2). Whereas the aortic flow waveforms demonstrated flow phases with peak systole (*A*), end systole (*B*), and end diastole (*C*),

the IVC flow was largely steady. Color contour plots displayed maps of velocity for the supraceliac and infrarenal levels at rest and during exercise at peak systole (*A*), end systole (*B*), and end diastole (*C*). The vessel lumen segmentations, as depicted by curves on the contour plots, revealed oval-shaped lumens in the IVC (thick-lined curve) compared with the more circular lumens in the aorta (thin-lined curve).

When the average hemodynamic quantities between the abdominal aorta and IVC for all subjects were compared, significant differences were found (Table 1). At the supraceliac level, mean blood flow rate was significantly higher in the aorta ( $2.9 \pm 0.6$  l/min) compared with the IVC ( $2.0 \pm 0.5$  l/min) at rest ( $P < 0.001$ ) and in the aorta ( $7.2 \pm 1.4$  l/min) compared with the IVC ( $6.5 \pm 1.4$  l/min) during exercise ( $P < 0.02$ ). At the infrarenal level, blood flow rate was greater in the IVC ( $1.2 \pm 0.5$  l/min) than in the aorta ( $0.9 \pm 0.4$  l/min) at rest ( $P < 0.01$ ). Furthermore, at the infrarenal level, mean wall shear stress was found to be significantly higher in the IVC ( $2.0 \pm 0.6$  dyn/cm<sup>2</sup>) compared with the aorta ( $1.3 \pm 0.6$  dyn/cm<sup>2</sup>) at rest ( $P < 0.005$ ) and not significantly higher in the IVC ( $7.5 \pm 1.9$  dyn/cm<sup>2</sup>) compared with the aorta ( $5.2 \pm 1.3$  dyn/cm<sup>2</sup>) during exercise. Lumen areas were also significantly larger in the infrarenal IVC ( $2.8 \pm 0.4$  cm<sup>2</sup>) compared with the infrarenal aorta ( $1.6 \pm 0.2$  cm<sup>2</sup>) at rest ( $P < 0.001$ ) and larger in the infrarenal IVC ( $3.2 \pm 0.7$  cm<sup>2</sup>) compared with the infrarenal aorta ( $1.4 \pm 0.4$  cm<sup>2</sup>) during exercise ( $P < 0.001$ ).

The data in Table 1 also illustrate the changes in average flow rates, wall shear stresses, and lumen areas in the supraceliac and infrarenal regions of the IVC from rest to exercise. The mean supraceliac flow rate increased from  $2.0 \pm 0.5$  l/min at rest to  $6.5 \pm 1.4$  l/min during exercise ( $P < 0.0005$ ), and the mean infrarenal flow increased from  $1.2 \pm 0.5$  l/min at rest to  $5.3 \pm 0.9$  l/min during exercise ( $P < 0.0005$ ). Mean wall shear stress increased from  $3.4 \pm 1.0$  l/min at rest to  $11.5 \pm 6.5$  l/min during exercise at the supraceliac level ( $P < 0.01$ ) and increased from  $2.0 \pm 0.6$  l/min at rest to  $7.5 \pm 1.9$  l/min during exercise at the infrarenal level ( $P < 0.0005$ ). Lumen area in the supraceliac region did not increase significantly from rest ( $2.3 \pm 0.9$  cm<sup>2</sup>) to exercise ( $2.5 \pm 1.4$  cm<sup>2</sup>); however, the infrarenal lumen area expanded from  $2.8 \pm 0.4$  cm<sup>2</sup> at rest to  $3.2 \pm 0.7$  cm<sup>2</sup> during exercise ( $P < 0.02$ ).

## DISCUSSION

There are some obvious qualitative differences between the hemodynamics in the abdominal aorta and IVC. The most noticeable difference is the lower pulsatility in the IVC compared with the aorta (Fig. 2). While the pulsatile blood flow in the aorta is driven by intermittent ejection of blood from the heart, by the time the blood reaches the capillary network and venous system, the pulse pressure has been dampened by the distensibility of the large arteries and viscous losses in the bloodstream and from the vessel wall. Also note that at rest, the infrarenal aortic segment

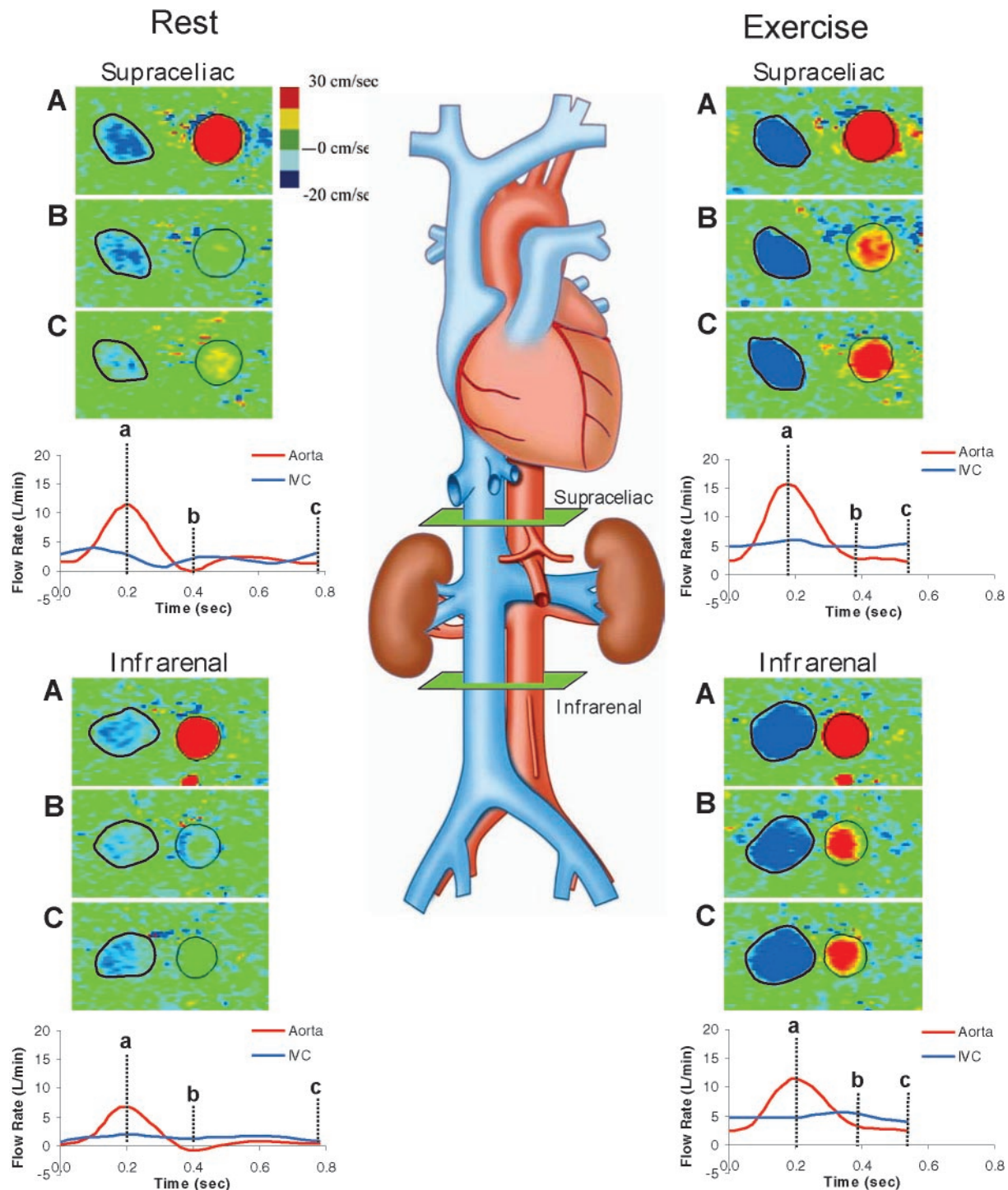


Fig. 2. Illustration of the human inferior vena cava (IVC) and abdominal aorta (*middle*) with measured flow rates and velocity maps for a representative subject at rest (*left*) and during dynamic lower limb exercise (*right*) at the supraceliac (*top*) and infrarenal (*bottom*) levels. The supraceliac image plane is just above the celiac artery on the aorta, and the infrarenal image plane is just below the renal arteries and veins. Volume flow rate curves demonstrated much greater pulsatility in the aorta than in the IVC for both locations and both physiological states. Note that, whereas there is reversal of flow in the infrarenal aorta under resting conditions, vena cava flow is always unidirectional. Color contours of measured velocity data are depicted at three times during the cardiac cycle: peak systole (A), end systole (B), and end diastole (C). Also shown are the lumen boundaries of the aorta (thin-lined curve) and IVC (thick-lined curve) computed by segmentation of the corresponding magnitude images.

Table 1. Comparison of mean blood flow rates, wall shear stresses, and lumen areas in the abdominal aorta and IVC at rest and during lower limb exercise

	Abdominal Aorta	IVC	Statistical Significance (P Values)
<i>Blood flow rate, l/min</i>			
Rest			
Supraceliac	2.9 +/- 0.6	2.0 +/- 0.5	<0.001
Infrarenal	0.9 +/- 0.4	1.2 +/- 0.5	<0.01
Exercise			
Supraceliac	7.2 +/- 1.4	6.5 +/- 1.4	<0.02
Infrarenal	5.6 +/- 1.1	5.3 +/- 0.9	
<i>Wall shear stress, dyn/cm<sup>2</sup></i>			
Rest			
Supraceliac	3.5 +/- 0.8	3.4 +/- 1.0	
Infrarenal	1.3 +/- 0.6	2.0 +/- 0.6	<0.005
Exercise			
Supraceliac	6.2 +/- 0.5	11.5 +/- 6.5	
Infrarenal	5.2 +/- 1.3	7.5 +/- 1.9	
<i>Lumen area, cm<sup>2</sup></i>			
Rest			
Supraceliac	2.1 +/- 0.4	2.3 +/- 0.9	
Infrarenal	1.6 +/- 0.2	2.8 +/- 0.4	<0.001
Exercise			
Supraceliac	2.0 +/- 0.4	2.5 +/- 1.4	
Infrarenal	1.4 +/- 0.4	3.2 +/- 0.7	<0.001

Values are means ± SD. Mean flow rate was significantly higher in the abdominal aorta compared with the inferior vena cava (IVC) at the supraceliac level at rest and during exercise; however, this was simply due to the lack of splanchnic drainage at this particular level of the IVC. Flow rate was higher in the IVC at the infrarenal level compared with the aorta at rest. Mean wall shear stress was statistically higher in the IVC compared with the abdominal aorta at the infrarenal level at rest. Lumen area at the infrarenal level was greater in the IVC than in the abdominal aorta at rest and during exercise.

experiences reverse flow at end systole (*time B*), whereas in the infrarenal IVC, the flow is unidirectional throughout the cardiac cycle (Fig. 2). There were no instances of reverse flow in the IVC for all subjects. The more oval-shaped lumens in the IVC compared with the aorta are a consequence of lower transmural pressures in the vena cava.

The flow distribution is also different between the abdominal aorta and IVC. Specifically, the supraceliac aorta carries more flow than the supraceliac IVC (Table 1). This is because in the abdominal aorta, the celiac, superior mesenteric, and renal arteries branch off between the chosen supraceliac and infrarenal slice locations of this study, whereas only the renal veins

empty into the IVC (Fig. 2). At basal conditions, it is expected that the sum of the digestive and renal arterial flow rates surpasses the renal venous flow alone because ~35% of abdominal aortic flow exits out through the celiac and superior mesenteric arteries (16). This agrees closely with our data, which show that the IVC flow at the supraceliac level at rest is 31% lower than that of the aortic flow (Table 1). The mean flow to the celiac, superior mesenteric, and renal arteries ( $2.1 \pm 0.5$  l/min) is significantly greater than that from the renal veins ( $0.7 \pm 0.6$  l/min) ( $P < 0.05$ ). The difference between these two values represents the hepatic portal flow. The average calculated hepatic portal flow of  $1.3 \pm 0.5$  l/min closely agrees with the 1.5 l/min reported by Germain et al. (9). Conversely, during exercise, there is no significant difference between the flow to the celiac, superior mesenteric, and renal arteries ( $1.6 \pm 0.7$  l/min) and from the renal veins ( $1.2 \pm 0.8$  l/min). This decrease in portal flow to  $0.4 \pm 0.7$  l/min is consistent with the finding that digestive arterial blood flow significantly decreases from rest to exercise (16, 27). Because the gastrointestinal flow enters a second capillary network in the liver via the hepatic portal vein, this type of analysis would be very useful for liver function assessment.

Mean wall shear stress was found to be significantly greater in the infrarenal IVC compared with the infrarenal aorta at rest. During exercise, a similar trend was observed, although it was not statistically significant. A theoretical explanation for the greater wall shear stress in the IVC comes from the mathematical solution of flow through a rigid tube with an elliptical cross section. Robertson et al. (20) showed with mathematical simulations that circumferentially averaged wall shear stress is higher in an elliptical tube compared with a cylinder, assuming that both have identical cross-sectional areas and volume flow rates. A possible physical explanation for this is that an elliptical lumen with a preserved cross-sectional area compared with a circular lumen has a larger lumen circumference. This greater circumference causes more viscous drag at the vessel wall, requiring a greater average driving pressure for an identical flow rate, which leads to a greater average wall shear stress.

The only significant differences in lumen cross-sectional area between the aorta and IVC were at the infrarenal level at rest and during exercise (Table 1). Whereas the abdominal aorta tapers in size inferiorly, our data show that the IVC tapers in size superiorly in

Table 2. Factor increase in mean flow rate, wall shear stress, and lumen area from rest to exercise

	Abdominal Aorta		IVC	
	Supraceliac	Infrarenal	Supraceliac	Infrarenal
Flow rate, l/min	2.48*	6.22*	3.25*	4.42*
Wall shear stress, dyn/cm <sup>2</sup>	1.77*	4.00*	3.38*	3.75*
Lumen area, cm <sup>2</sup>	0.95	0.88	1.09	1.14*

Flow rate and wall shear stress increased significantly for the supraceliac and infrarenal locations in the abdominal aorta and IVC. Lumen area did not increase significantly in the aorta or at the supraceliac level for the IVC, but it increased significantly at the infrarenal level in the inferior vena cava. \*Statistical significance ( $P < 0.05$ ).

the abdomen at rest ( $P < 0.005$ ) and during exercise ( $P < 0.001$ ) (Table 1). This tapering in the superior direction, to the authors' knowledge, has not been previously reported and may be important when considering deployment of venous stents, grafts, and filters.

Mean flow rate and wall shear stress both increased from rest to exercise for the supraceliac and infrarenal segments in both the aorta and IVC (Table 2). While there is a discrepancy between the factor increase (exercise quantity/rest quantity) in wall shear stress from rest to exercise compared with the factor increase in flow rate from rest to exercise in the aorta (27), the ratios for wall shear stress and flow rate for the IVC are much closer (Table 2). According to pulsatile flow theory through a rigid tube, mean wall shear stress should be linearly proportional to the mean flow rate, and these exercise-to-rest ratios should be the same (32). The better agreement may be due to the more steady nature of flow in the IVC, potentially causing lower errors in velocity gradient estimation at the lumen wall. Steep spatial velocity gradients in the aorta, along with vessel motion during the cardiac cycle, could result in image blurring, which causes underestimation of wall shear stress in the aorta (27). These errors can be exacerbated during exercise due to increased heart rate and hence temporal blurring of data (18). Lumen area significantly increased at the infrarenal level in the IVC from rest to exercise (Table 2). An explanation could be that during the exercise, the higher driving pressure and flow dilate the vessel lumen.

Note that while the cine phase-contrast MRI data we acquired in this study were temporally resolved, we reported temporally averaged quantities. The image acquisitions were resolved for the cardiac cycle; however, they were respiratory compensated rather than respiratory resolved. For this particular respiratory compensation algorithm (7), the image data most closely represent end-expiration because the center of  $k$ -space was acquired near end-expiration. Fredrickson et al. (7) showed that at end-expiration, portal venous flow rate is not statistically different from its respiratory-averaged flow rate (7).

In summary, we investigated the flow environment of the IVC at the supraceliac and infrarenal levels at rest and during dynamic lower limb exercise using cine phase-contrast MRI techniques. In general, mean infrarenal IVC flow rate and wall shear stress were higher than in the aorta. Also, flow reversal, present in the infrarenal aorta at rest, is not observed in the IVC. These IVC hemodynamic properties are hypothesized to be advantageous compared with those in the aorta, which is consistent with the lower incidence of disease in the IVC compared with the abdominal aorta. We also examined the differences in flow distribution between the aorta and IVC, tapering of the IVC in the abdominal region, and the effects of exercise on flow rate, wall shear stress, and lumen area. These data add to our understanding of the circulatory system as well as providing information useful for clinical purposes.

Finally, the methods that were developed for this study could potentially improve diagnosis of vascular diseases and assessment of their treatments.

The authors acknowledge the assistance of Beverly Tang, Leandro Espinosa, David Parker, Anna McVittie, and Mary Draney of the Department of Mechanical Engineering and Dr. Thomas Brosnan, Dr. Norbert Pelc, Claudia Cooper, and Ann Taylor of the Department of Radiology at Stanford University.

This work was supported by the Lucas Foundation and National Institutes of Health Grant P41-RR-09784. C. Cheng was supported with a Whitaker Foundation predoctoral fellowship.

## REFERENCES

1. Berne RM and Levy MN. *Cardiovascular Physiology*. St. Louis, MO: Mosby-Year Book, 1997.
2. Caro CG, Fitz-Gerald JM, and Schroter RC. Atheroma and arterial wall shear: observation, correlation and proposal of a shear-dependent mass transfer mechanism for atherogenesis. *Proc R Soc Lond B Biol Sci* 177: 109–159, 1971.
3. Cheng CP, Parker D, and Taylor CA. *Wall Shear Stress Quantification from Magnetic Resonance Imaging Data Using Lagrangian Interpolation Functions*. Park City, UT: ASME Summer Bioengineering Meeting, 2001, p. 795–796.
4. Cheng CP, Parker D, and Taylor CA. Quantification of wall shear stress in large blood vessels using Lagrangian interpolation functions with cine phase-contrast magnetic resonance imaging. *Ann Biomed Eng* 30: 1020–1032, 2002.
5. Fogel MA, Weinberg PM, Rychik J, Hubbard A, Jacobs M, Spray TL, and Haselgrove J. Caval contribution of flow in the branch pulmonary arteries of fontan patients with a novel application of magnetic resonance presaturation pulse. *Circulation* 99: 1215–1221, 1999.
6. Frank H, Globits S, Glogar D, Neuhold A, Kneussl M, and Mlczoch J. Detection and quantification of pulmonary artery hypertension with MR imaging. *Am J Roentgenol Radium Ther* 161: 27–31, 1993.
7. Fredrickson JO, Wegmuller H, Herfkens RJ, and Pelc NJ. Simultaneous temporal resolution of cardiac and respiratory motion in MR imaging. *Radiology* 195: 169–175, 1995.
8. Friedman MH, Hutchins GM, and Barger CB. Correlation between intimal thickness and fluid shear in human arteries. *Atherosclerosis* 39: 425, 1981.
9. Germain P, Baruthio J, Wecker D, Roul G, Koegler A, Mossard JM, Bareiss P, Chambron J, and Sacrez A. [Dynamic cartography of flow patterns by cine-MRI presentation of the technique and preliminary results for major vessels.] *Ann Cardiol Angeiol (Paris)* 42: 61–71, 1993.
10. Gill RW. Measurement of blood flow by ultrasound: accuracy and sources of error. *Ultrasound Med Biol* 11: 625–641, 1985.
11. Goldhammer E, Mesnick N, Abinader EG, and Sagiv M. Dilated inferior vena cava: a common echocardiographic finding in highly trained elite athletes. *J Am Soc Echocardiogr* 12: 988–993, 1999.
- 11a. Gow BS. Circulatory correlates: vascular impedance, resistance, and capacity. In: *Handbook of Physiology. The Cardiovascular System. Vascular Smooth Muscle*. Bethesda, MD: Am. Physiol. Soc., 1980, sect. 2, vol. II, chapt. 14, p. 353–408.
13. Kluckow M and Evans N. Low systemic blood flow and hyperkalemia in preterm infants. *J Pediatr* 139: 227–232, 2001.
14. Ku D, Giddens D, Zarins C, and Glagov S. Pulsatile flow and atherosclerosis in the human carotid bifurcation: positive correlation between plaque location and low oscillating shear stress. *Arteriosclerosis* 5: 293–302, 1985.
15. Moore J and Ku D. Pulsatile velocity measurements in a model of the human abdominal aorta under simulated exercise and postprandial conditions. *J Biomech Eng* 116: 107–111, 1994.
16. Moore J, Ku D, Zarins C, and Glagov S. Pulsatile flow visualization in the abdominal aorta under differing physiological conditions: implications for increased susceptibility to atherosclerosis. *J Biomech Eng* 114: 391–397, 1992.
17. Pedersen E, Kozerke S, Ringgaard S, Scheidegger MB, and Boesiger P. Quantitative abdominal aortic flow measure-

- ments at controlled levels of ergometer exercise. *Magn Reson Imaging* 17: 489–494, 1999.
18. **Pelc NJ, Herfkens RJ, Shimakawa A, and Enzmann DR.** Phase contrast cine magnetic resonance imaging. *Magn Reson Q* 7: 229–254, 1991.
  19. **Pelc NJ, Sommer FG, Li KC, Brosnan TJ, Herfkens RJ, and Enzmann DR.** Quantitative magnetic resonance flow imaging. *Magn Reson Q* 10: 125–147, 1994.
  20. **Robertson MB, Kohler U, Hoskins PR, and Marshall I.** Flow in elliptical vessels calculated for a physiological waveform. *J Vasc Res* 38: 73–82, 2001.
  21. **Rothe CF.** Venous system: physiology of the capacitance vessels. In: *Handbook of Physiology: the Cardiovascular System*, edited by Shepherd JT and Abboud FM. New York: Oxford Univ. Press, 1983, sect. 2, p. 397–452.
  22. **Schalet B, Taylor C, Harris E, Herfkens R, and Zarins C.** Quantitative assessment of human aortic blood flow during exercise. *Surgical Forum XLVIII*: 359–362, 1997.
  23. **Schanzer H, Younis C, Train J, and Peirce EC.** Therapeutic implications of phlebographic obstruction in chronic venous stasis. *J Cardiovasc Surg (Torino)* 31: 173–177, 1990.
  24. **Schnittler H, Schmandra T, and Drenckhahn D.** Correlation of endothelial vimentin content with hemodynamic parameters. *Histochem Cell Biol* 110: 161–167, 1998.
  25. **Sethian JA.** *Level Set Methods and Fast Marching Methods*. Cambridge, UK: Cambridge Univ. Press, 1999.
  26. **Smith HJ, Grottum P, and Simonsen S.** Ultrasonic assessment of abdominal venous return. Effect of cardiac action and respiration on mean velocity pattern, cross-sectional area and flow in the inferior vena cava and portal vein. *Acta Radiol* 26: 581–588, 1985.
  27. **Taylor CA, Cheng CP, Espinosa LA, Tang BT, Parker D, and Herfkens RJ.** In vivo quantification of blood flow and wall shear stress in the human abdominal aorta during lower limb exercise. *Ann Biomed Eng* 30: 402–408, 2002.
  28. **Taylor CA, Hughes TJR, and Zarins CK.** Effect of exercise on hemodynamic conditions in the abdominal aorta. *J Vasc Surg* 29: 1077–1089, 1999.
  29. **Umemoto Y, Nishi S, Shindoh M, and Asada A.** Venous blood flow measurement by determination of change in venous hemoglobin saturation. *Crit Care Med* 28: 3181–3184, 2000.
  30. **Van Rossum AC, Sprenger M, Visser FC, Peels KH, Valk J, and Roos JP.** An in vivo validation of quantitative blood flow imaging in arteries and veins using magnetic resonance phase-shift techniques. *Eur Heart J* 12: 117–126, 1991.
  31. **Wang KC.** *Level Set Methods for Computational Prototyping with Application to Hemodynamic Modeling* (PhD Dissertation). Stanford, CT: Stanford University, 2001.
  32. **Womersley J.** Method for the calculation of velocity, rate of flow and viscous drag in arteries when the pressure gradient is known. *J Physiol* 127: 553–563, 1955.
  33. **Zarins CK, Giddens DP, Bharadvaj BK, Sottiurai VS, Mabon RF, and Glagov S.** Carotid bifurcation atherosclerosis: quantitative correlation of plaque localization with flow velocity profiles and wall shear stress. *Circ Res* 53: 502–514, 1983.

